2010 IEEE/ASME International Conference on
Advanced Intelligent Mechatronics
Montréal, Canada, July 6-9, 2010

Experimental demonstration of a swimming robot propelled by the gradient field of a Magnetic Resonance Imaging (MRI) system

Viviane Lalande, *Student member IEEE*, Frederick P. Gosselin, Sylvain Martel, *Senior Member, IEEE*

Abstract— **Travelling inside the human body is an on-going scientific challenge. In this paper, we propose a new way of propelling robots inside the human body for gastro-intestinal applications actuated with the gradient field of an unmodified Magnetic Resonance Imaging (MRI) system. The robot is composed of a soft ferromagnetic head and a plastic tail attached together. This assembly is then placed in a bath of water inside an MRI system. The main field of the MRI is used to magnetize the head of the device while a gradient field is used to put the robot into motion. The oscillating magnetic gradient creates a force perpendicular to the direction of swimming and as the device drifts in this direction, the lift produced on its tail moves it in the forward direction. A study varying the length of the tail of the robot from 20mm to 80mm, the frequency applied and the amplitude of the gradient has been conducted and is developed in the following.**

I. Introduction

Miniaturization of medical devices offers the promises of minimally invasive treatments such as drug delivery [1], endoscopy [2] or microsurgery [3]. Much of the potential of the miniaturization lies in concept of micro-devices travelling inside the human body. In order to reach the smallest sites, the use of untethered devices is a necessity. The use of externally generated magnetic fields allows to power and control micro-robots without the need for energy storage or complex miniaturized control systems. Most applications of magnetic steering use one of the three following modes of propulsion [4]: (i) a magnetic field uniform in space and oscillating in time applies a torque on a head which is transformed into a flapping motion by a flexible tail [5]; (ii) a rotating field applied on a magnetic head rotates a helical tail [6]; (iii) a magnetic gradient directly pulls the micro-robot [7].

Most magnetic micro-robots are designed to be steered with permanent magnets or coils specifically designed for control and propulsion. However, it has been shown that a ferromagnetic bead can be propelled and steered by pulling on it using the magnetic gradients generated with an unmodified Magnetic Resonance Imaging (MRI) apparatus [7]. Moreover, another design of biomedical micro-devices powered wirelessly by an MRI system has been demonstrated. The propulsion is generated from embedded coils where an electric current, powered by radio-frequencies from an MRI system, interacts with the main field of the MRI [8]. MRI apparatus offer a great advantage for magnetic propulsion as they are already widely available in most hospitals. No costly new platform is thus required to perform micro-surgery.

The purpose of this paper is to introduce a new way to propel and control a device using an unmodified MRI system and its magnetic properties. A micro-robot propelled by a lift-based swimming mechanism was built and tested in an MRI apparatus. This robot is composed of a head made of a magnetic bead attached to a flexible tail which acts like the keel of a sailboat. Inside the MRI apparatus, the bead is magnetized along the main axis of the MRI system by the mean field and an alternating gradient field produced by Golay-type coils and perpendicular to the main field is applied. The oscillating magnetic gradient creates a force perpendicular to the direction of swimming and as the device drifts in this direction, the lift produced on its tail moves it in the forward direction as depicted in Fig 1. The mode of propulsion we present here is different from that used by [5] which requires a rotating magnetic field impossible to create in an MRI system whereas our system is propelled by magnetic gradients. The lift-based mode of propulsion of our device, in its current dimensions, could be developed for gastro-intestinal applications or even for swimming in the largest arteries where the Reynolds number [9] is relatively large.

In the following sections, the details of the experiments are given and the results showing the performances of the device are presented.

II. Experimental setup

A. MRI system settings

An MRI system is a high resolution imaging apparatus widely exploited in hospitals. Its technology is based on nuclear magnetic resonance (NMR) theory. An RF pulse is sent to excite a specific nucleus, targeted spatially by using magnetic gradients [10]. In the current project, these

Manuscript received February 14, 2010. This work was supported in part by the Canadian Foundation for the innovation (FCI) in part by the Canada Research Chair (CRC) and in part by the Natural Sciences and Engineering Research Council of Canada (NSERC).

V.Lalande (viviane.lalande@polymtl.ca) and F. P. Gosselin (frederick.gosselin@polymtl.ca) are with the Nano-Robotics laboratory, École Polytechnique de Montréal (EPM).

S. Martel (corresponding author) is with the Nano-Robotics laboratory, Department of Computer and Software Engineering and the Institute of Biomedical Engineering. École Polytechnique de Montréal (EPM), Montréal, H3C 3A7 Canada (phone : 514 340-4711 ext. 5098; e-mail: sylvain.martel@polymtl.ca).

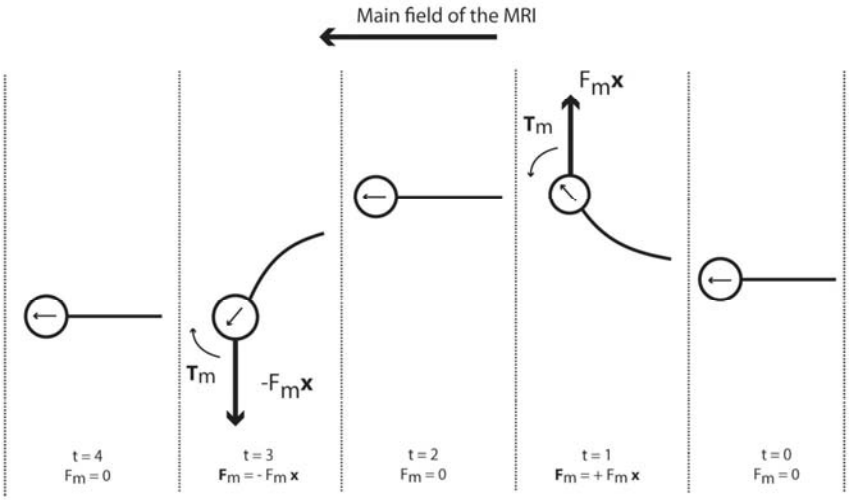

Fig.1: Representation of the behavior of the robot under the alternating field where Fm is the magnetic force produced by the alternating gradient, Tm is the torque induced by the anisotropy, and t is an arbitrary time. Arrows inside the ball represent the magnetization direction.

gradients are used to generate magnetic forces for propulsion.

The permanent field of the MRI system magnetizes the ferromagnetic material of the swimming robot and an oscillating gradient is applied in the direction perpendicular to the direction of swimming. The resulting force in the direction of the gradient induces a drifting motion of the swimmer. As the swimmer gains a relative velocity with respect to the still fluid, the flow on the tail creates a lift force which propels the swimmer forward as depicted in Figure 1.

The coils of an MRI apparatus are designed for imaging and thus are optimized for high frequency and short loads while for propulsion applications, low frequency and strong loads are desirable. To adapt our propulsion problem to this constraint of the apparatus, we limit the duty cycle of the gradient coils to 30%, meaning that during 70% of the period, no propulsion gradient is applied and higher frequency imaging gradients could be applied. On top of the duty cycle, three parameters have been set in the MRI system: the frequency, the amplitude and the direction of the gradient field. The oscillating propulsion gradient is applied with a frequency *f*, amplitude ∇B and takes the form of a square wave as depicted in Fig. 2. The main field of the MRI apparatus is constant in the z-direction and the gradient is applied alternatively along the plus and minus x-direction (Fig 3).

B. Materials

The swimming magnetic robot is composed of a head made of a carbon steel alloy suspended by a floater made of polystyrene foam and attached to a tail made of a thin flexible acetate sheet. Carbon steel is a soft ferromagnetic material which allows easier reorientation of the magnetization than hard ferromagnetic materials. The magnetic head is shaped as a sphere in order to minimize shape-anisotropy. This is a requirement when working in an MRI system in order not to be constrained with the direction of magnetization. However there is always a small anisotropy which subsides due to the orientation of the crystals, and thus the material still has a slight magnetization-direction preference. When the material is not aligned with the MRI system, a magnetic torque T_m [11] appears:

$$\vec{T}_m = V.\vec{M} \times \vec{B} \quad , \tag{1}$$

where V is the volume of magnetic matter, ***M*** is the magnetization of the material and ***B*** is the field of the MRI system. Because the anisotropy was significant, the tail was attached to the magnetic head inside the MRI apparatus so as to align the tail and the preferred magnetization direction along the main magnetic field in the *z*-axis. In this way, the swimmer always feels a torque realigning it with the main magnetic field of the MRI system and keeps its direction very accurately as it is depicted in Fig. 1.

Symbol	Quantity	Value
m	Ball mass	0.442g
d	Ball diameter	4.75mm
	Ball material	1010/1020 C/S
M	Ball magnetization in a 1.5T MRI system	1 248 000 A/m
Hc	Ball Coercitive field	3820 A/m
EI	Tail bending moment	$6.95.10^{-6}$ N.m²
L	Tail length	From 20mm to 80mm
w	Tail width	10mm
e	Tail thickness	0.1mm
	Tail material	Transparent plastic sheet

Table 1. Material properties of the magnetic swimming device

The swimming robot has slightly positive buoyancy as the head is attached to a floater made of polystyrene foam and only barely protrudes from the surface of the water of the bath it is immersed in. The tail is fastened to the head and its length is varied throughout the experiment. The properties of the head and the tail are summarized in Table 1. The robot swims horizontally in a bath of water placed in the main field of a Siemens Sonata 1.5T MRI system. An

MRI compatible camera is placed on the top of the bath and records the motions of the device (Fig. 4).

C. Magnetic force

An oscillating gradient is applied along the *x*-direction creating a magnetic force on the head of the device proportional to the volume of magnetic material, its magnetization in a 1.5T MRI system and the gradient:

$$\vec{F}_{magn} = V.(\vec{M}.\nabla)\vec{B}, \quad (2)$$

where V is the volume of our magnetic ball, M its magnetization and ∇B the gradient applied.

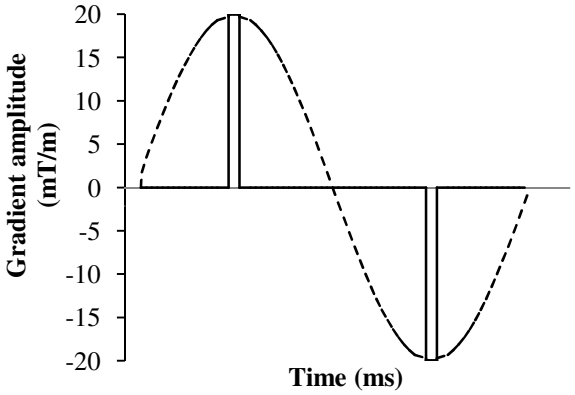

Fig. 2: Schematic representation of the duty cycle of the MRI system (solid line) as compared with a sinusoidal function (dashed line).

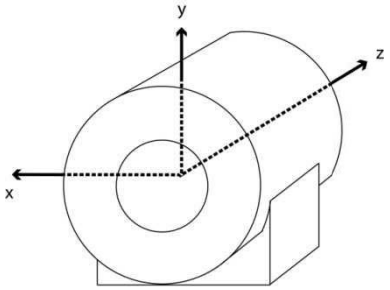

Fig. 3: Schematic representation of an MRI system with its axes. The reference point is located at the center of the bore.

III. Results

Two sets of experimental runs were conducted for various lengths of the tail to test the swimming ability of the robot: (i) for various forcing frequencies of the oscillating gradient between 0.2 Hz and 3.15Hz; (ii) for incrementing amplitude of the gradient with 5mT/m steps from 5mT/m to 24mT/m, (which is the maximum load acceptable on the coils of the MRI system for the given duty cycle).

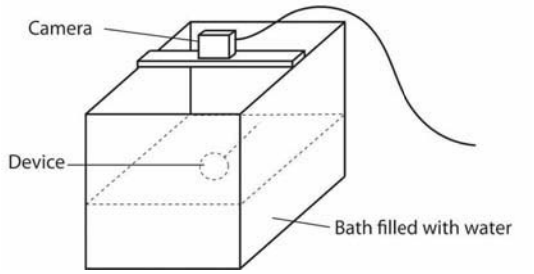

Fig. 4: Schematic representation of the experimental setup.

A. Behavior

The paths followed by the device have been recorded (Fig. 5). We aim to move the device from a place to another. The shortest distance is a straight line (dotted lines on Fig.5), but in this study, to move the device from right to left (Fig. 5) we apply a transverse magnetic gradient creating an amplitude. It was shown that, the lengthier the tail is, the more it has a sinusoidal path. The bigger the surface of the tail is, the slower it becomes to make a rotation because it entrains more water.

The velocity has also been recorded showing that the square wave forcing function (Fig.2) induces a square wave velocity along ***x*** (Fig.6). Meanwhile, the trace of the velocity along ***z*** is smoother and a phase shift between the highest value along ***x*** and along ***z*** is observed.

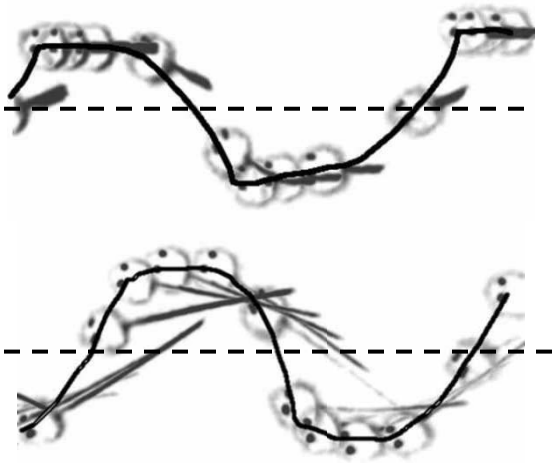

Fig. 5: Path decomposition for a 20mT/m amplitude and a 0.2Hz frequency of a 2cm tail length (a) and an 8cm tail length (b). The white circles are the polystyrene heads in which the magnetic ball is located. The black thick lines are tails and the long black line is the path.

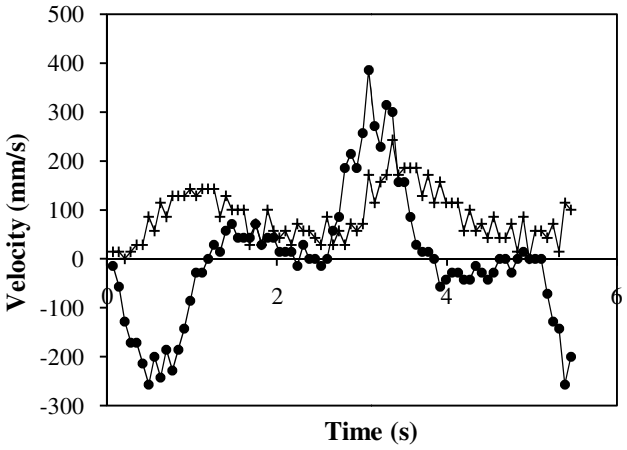

Fig. 6: Velocity of the device is a function of the time and the behavior depends on the gradient field applied. —●— Along ***x***, —+— along ***z***.

B. Velocity and amplitude data

The average velocity of the robot measured over a distance of 14.4 cm for various values of tail length L is shown in Fig. 5 versus the frequency f of the alternating force applied by the MRI system coils for a magnetic gradient of 20

mT/m. The maximum average velocity recorded is 42.4 mm/s for a specimen with a tail of 3 cm at a frequency of 0.5 Hz. For every tail length, the relation of the average velocity with the frequency of excitation is similar: at low frequency, the velocity reaches a plateau between 30 and 40 mm/s and the longer the tail is, the lower the frequency must be to reach the plateau. Over the range of frequencies studied, the plateau spreads over a wider range of frequencies for shorter tail lengths.

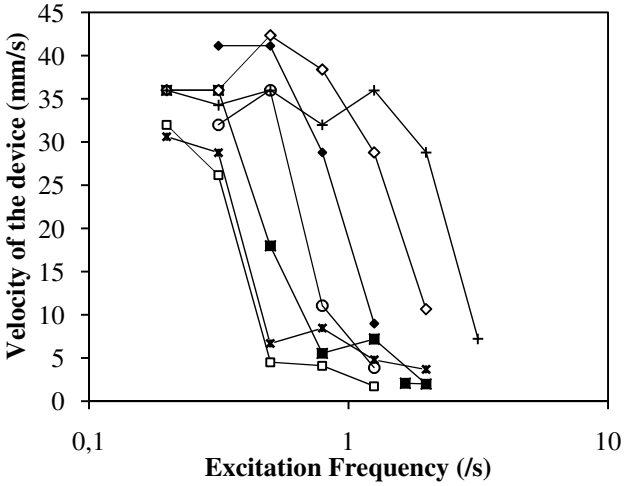

Fig. 7: Velocity of the device as a function of the excitation frequency for varying tail length : 8cm, 7cm, 6cm, 5cm, 4cm, 3cm, 2cm. The magnitude of the force applied is 1.4mN.

The data of the second set of runs showing the measured averaged velocity and amplitude of the swimmer versus the magnitude of the force applied are shown in Fig. 8 (a) for various tail lengths. Here, the maximum average velocity recorded is 42 mm/s for the 2cm, 4cm, and 5cm long specimen. Again, a trend is highly discernible for the various lengths of tail tested. For every specimen, for lower values of the magnitude of the oscillating force applied, the velocity increases linearly with the force. However, when the gradient exceeds 15mT/m (i.e 1.05 mN), a plateau is reached and for any tail length tested, the swimmer does not move faster as the force is increased.

On Fig. 8 (b) is plotted the transverse amplitude of the fish against the magnetic force applied at 0.2Hz frequency. The amplitude shows a linear behavior for each length. At 24mT/m where the velocity plateau ends (Fig.8 (b)), the 2cm-tail device reaches the highest velocity and has the lowest amplitude.

C. Efficiency

We evaluate the efficiency of the swimming of the device by calculating the ratio of the kinetic energy of device divided by the work done by the magnetic field to move the swimmer across the water bath:

$$\eta = \frac{E_C}{W} = \frac{\frac{1}{2}mU^2}{2F_m A f \frac{l}{U}} = \frac{mU^3 l}{4F_m f A}, \quad (3)$$

where m, U and A are respectively the mass, the average velocity and the transverse amplitude of motion of the swimmer, F_m and f are the magnitude and the frequency of the magnetic force, and where l is the length of the water bath.

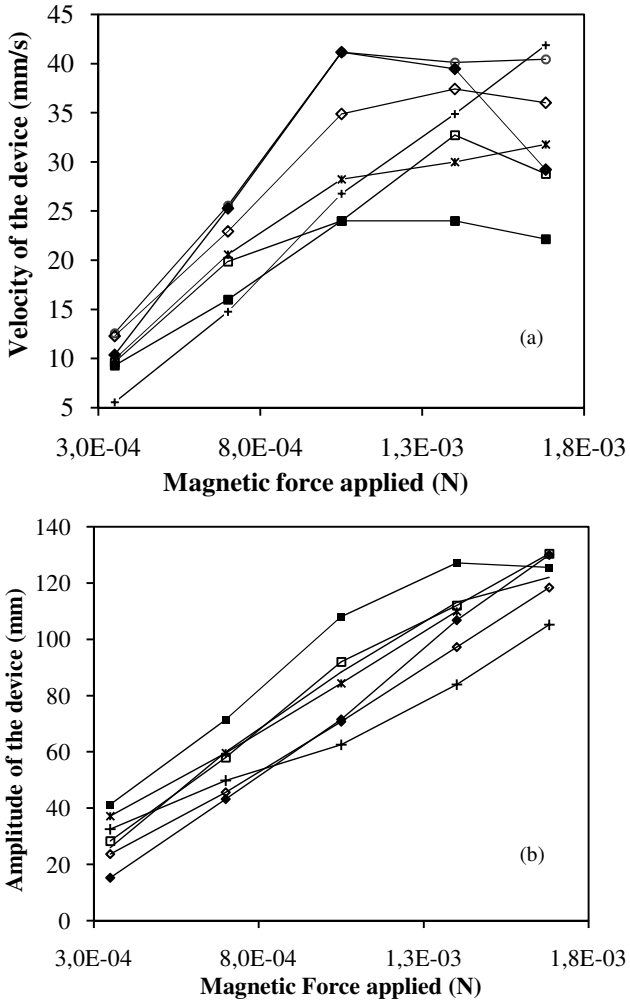

Fig 8: Velocity (a) and amplitude (b) of the device as a function of the magnetic force applied for varying tail length: 8cm, 7cm, 6cm, 5cm, 4cm, 3cm, 2cm. The forcing frequency is 0.2Hz. :

In flapping propulsion, the ratio of the beating frequency, beating amplitude and cruising velocity has a strong influence on the efficiency of locomotion. This ratio is defined by the Strouhal number:

$$s_t = \frac{fA}{U}, \quad (4)$$

where f is the applied frequency, A is the full amplitude and U is the velocity.

Most swimming and flying animals cruise at a velocity corresponding to a Strouhal number between 0.2 and 0.4 [12]. Correspondingly, we compare in Fig. 9 the efficiency of the locomotion of our swimming robot to the Strouhal number corresponding to their stroke. It is shown that by far the best efficiency attained by our device occurs in the range of Strouhal numbers of 0.25 and 0.60. This peak of efficiency occurs when the shed vortices shows a maximum amplification in the wake [13].

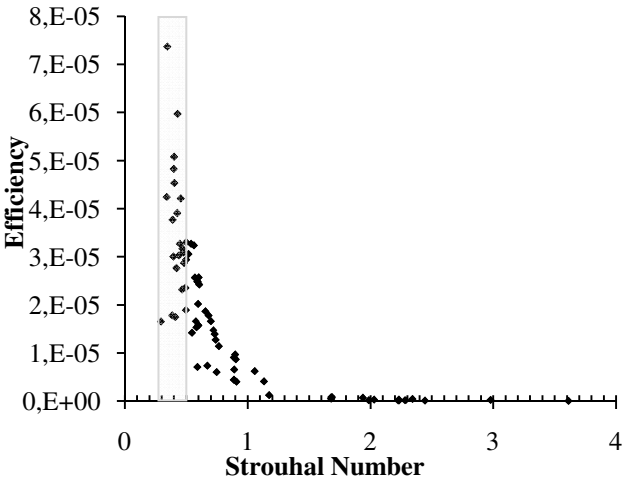

Fig. 9: Efficiency of the swimming device in function of the Strouhal number of its stroke.

IV. Discussion

The experiments presented were conducted along one direction (*z*-axis) as the material tested had crystalline anisotropy. The latter induces a preferred orientation of the robot in the MRI system which acts as a rotational spring. Once the ball (acting as the main body of the robot) rotated away from alignment, it induced a torque to realign the ball along *z*. However, with a material presenting better isotropy (disappearance of the torque) like a balloon of ferrofluid, it would be possible to steer the robot in any directions.

However, the anisotropy helps to stabilize the motion of the robot. Without this anisotropy, it may be necessary to perform a close loop control on the robot during travel.

The chosen way of propelling is one solution among others. For comparison purposes, the robot was also tested in a simple traction test without any transverse gradient (Fish z) and showed a rectilinear path and a velocity 53% greater than with the alternating transverse gradient (Fish x). The same experiment was conducted with a single ball without any tail (Bead z) and showed a chaotic path and a velocity 61% greater than the robot presented in the paper (Fish x). Velocity, amplitude and efficiency of each way of propelling presented are depicted in Table 2. These three solutions all have their advantages and their drawbacks. On the one hand, the first two solutions, Fish x and Fish z, may be slower than the third one, Bead z, but are useful in case of an upgraded MRI where the number of coil is reduced. Indeed, a path in a 2-dimentional space can be achieved with only one coil. On the other hand, the third solution composed of the single ball which is the quickest and the smallest needs a retroaction loop like presented in [14] in order to make the path less chaotic. Furthermore, the 3-dimentional coil is essential as well.

V. Conclusion

A magnetic ball-and-tail swimming robot was successfully propelled inside a water bath in an MRI system through the application of an oscillating transverse magnetic gradient. This study proves that a new way of propelling devices inside an MRI system is possible and this model is partially optimized. Indeed, the most efficient frequency is known for each length as well as the magnetic force needed to induce a motion. Tests showed that the most efficient and the fastest fish is that with a 2cm- tail, with 24mT/m gradient and 0.2Hz frequency. It has both the lowest amplitude and the greatest speed. The efficiency of the swimming of the device was maximized at the same values of Strouhal number as those of swimming animals.

Test	Speed (mm/s)	Amplitude (mm)	Efficiency
Fish x	31.79	115	$1.32.10^{-5}$
Fish z	109.92	0.40	$5.75.10^{-4}$
Bead z	130.90	38.40	$2.77.10^{-3}$

Table 2. Tests comparison of different modes of propulsion.
Tests are performed at 0.4Hz frequency, 24mT/m gradient field and 8cm tail length when a tail is used.
Fish x is the test performed with a gradient field applied along ***x*** (oscillating). ***Fish z*** has a gradient field applied along *z* (pulling). ***Bead z*** is the same test as F***ish z*** but without a tail.

Further work will aim to combine these results with a theoretical model while running new experiments varying other parameters such as the width and thickness of the tail as well as the material and ball size. A proper dimensional analysis of the problem could allow identifying the relationship between all the parameters and the velocity of the device. It would also be interesting to change the duty cycle of the MRI system by reducing the amplitude but increasing the application time of the magnetic gradient.

Acknowledgment

The authors wish to acknowledge M. Vonthron for his help with the MRI system along with the Nanorobotic lab staff of the "Ecole Polytechnique de Montréal" for its support.

References

[1] P. Pouponneau, J. Leroux, and S. Martel, "Magnetic nanoparticles encapsulated into biodegradable microparticles steered with an upgraded magnetic resonance imaging system for tumor chemoembolization," *Biomaterials*, vol. 30, (no. 31), pp. 6327-6332, 2009.

[2] M. Quirini, S. Scapellato, A. Menciassi, P. Dario, F. Rieber, C. Ho, S. Schostek, and M. Schurr, "Feasibility proof of a legged locomotion capsule for the GI tract," *Gastrointestinal Endoscopy*, 2008.

[3] J. Edd, S. Payen, B. Rubinsky, M. Stoller, and M. Sitti, "Biomimetic propulsion for a swimming surgical micro-robot," in Book Biomimetic propulsion for a swimming surgical micro-robot, *Series Biomimetic propulsion for a swimming surgical micro-robot*, 2003, pp. 2583-2588.

[4] J. Abbott, K. Peyer, L. Dong, and B. Nelson, "How should microrobots swim?," *The International Journal of Robotics Research*, vol. 28, (no. 11-12), pp. 1434, 2009.

[5] S. Sudo, S. Segawa, and T. Honda, "Magnetic swimming mechanism in a viscous liquid," *Journal of intelligent material systems and structures*, vol. 17, (no. 8), pp. 729-736, 2006.

[6] T. Honda, K. Arai, and K. Ishiyama, "Micro swimming mechanisms propelled by external magnetic fields," *IEEE Transactions on Magnetics*, vol. 32, (no. 5), pp. 5085-5087, 1996.

[7] J. Mathieu, G. Beaudoin, and S. Martel, "Method of propulsion of a ferromagnetic core in the cardiovascular system through magnetic gradients generated by an MRI system," *IEEE Transactions on Biomedical Engineering*, vol. 53, (no. 2), pp. 292-299, 2006.

[8] G. Kósa, P. Jakab, F. Jólesz, and N. Hata, “Swimming capsule endoscope using static and RF magnetic field of MRI for propulstion,” in Book Swimming capsule endoscope using static and RF magnetic field of MRI for propulstion, *Series Swimming capsule endoscope using static and RF magnetic field of MRI for propulstion*, Editor ed.^eds., City, 2008, pp. 2922–2927.

[9] S. Childress, *Mechanics of swimming and flying*: Cambridge Univ Pr, 1981.

[10] J. Hornak, “The basics of MRI,” [Online]. Available: *http://www.cis.rit.edu/htbooks/mri* Vol 8.

[11] E. Du Tremolet De Lacheisserie. (2000) “Magnétisme I: Fondements” (EDP sciences). [Book]. Tome I.

[12] G. Taylor, R. Nudds, and A. Thomas, “Flying and swimming animals cruise at a Strouhal number tuned for high power efficiency,” *Nature*, vol. 425, (no. 6959), pp. 707-711, 2003.

[13] J. Anderson, K. Streitlien, D. Barrett, and M. Triantafyllou, “Oscillating foils of high propulsive efficiency,” *Journal of Fluid Mechanics*, vol. 360, pp. 41-72, 1998.

[14] S. Martel, J. Mathieu, O. Felfoul, A. Chanu, E. Aboussouan, S. Tamaz, P. Pouponneau, G. Beaudoin, G. Soulez, and M. Mankiewicz, “Automatic navigation of an untethered device in the artery of a living animal using a conventional clinical magnetic resonance imaging system,” *Applied Physics Letters*, vol. 90, pp. 114105, 2007.